

## Article

# MgO Nano-Catalyzed Biodiesel Production from Waste Coconut Oil and Fish Oil Using Response Surface Methodology and Grasshopper Optimization

Impha Yalagudige Dharmegowda <sup>1</sup>, Lakshmidhevamma Madarakallu Muniyappa <sup>1,2</sup>, Parameshwara Siddalingaiah <sup>3</sup>, Ajith Bintravalli Suresh <sup>4</sup>, Manjunath Patel Gowdru Chandrashekarappa <sup>5,\*</sup> and Chander Prakash <sup>6,7,\*</sup>

<sup>1</sup> Department of Mechanical Engineering, Government Engineering College, Visvesvaraya Technological University, Kushalnagara 571234, India

<sup>2</sup> Department of Mechanical Engineering, Government Engineering College, Visvesvaraya Technological University, Challakere 577522, India

<sup>3</sup> Department of Mechanical Engineering, JNN College of Engineering, Visvesvaraya Technological University, Shivamogga 577204, India

<sup>4</sup> Department of Mechanical Engineering, Sahyadri College of Engineering and Management, Visvesvaraya Technological University, Mangalore 575007, India

<sup>5</sup> Department of Mechanical Engineering, PES Institute of Technology and Management, Visvesvaraya Technological University, Shivamogga 577204, India

<sup>6</sup> School of Mechanical Engineering, Lovely Professional University, Phagwara 144411, India

<sup>7</sup> Division of Research and Development, Lovely Professional University, Phagwara 144411, India

\* Correspondence: manju09mpm05@gmail.com (M.P.G.C.); chander.mechengg@gmail.com (C.P.); Tel.: +91-9844859032 (M.P.G.C.)



**Citation:** Dharmegowda, I.Y.; Muniyappa, L.M.; Siddalingaiah, P.; Suresh, A.B.; Gowdru Chandrashekarappa, M.P.; Prakash, C. MgO Nano-Catalyzed Biodiesel Production from Waste Coconut Oil and Fish Oil Using Response Surface Methodology and Grasshopper Optimization. *Sustainability* **2022**, *14*, 11132. <https://doi.org/10.3390/su141811132>

Academic Editor: Changhyun Roh

Received: 9 August 2022

Accepted: 30 August 2022

Published: 6 September 2022

**Publisher's Note:** MDPI stays neutral with regard to jurisdictional claims in published maps and institutional affiliations.



**Copyright:** © 2022 by the authors. Licensee MDPI, Basel, Switzerland. This article is an open access article distributed under the terms and conditions of the Creative Commons Attribution (CC BY) license (<https://creativecommons.org/licenses/by/4.0/>).

**Abstract:** In India, a densely populated country, fossil fuel depletion affects the energy sector that fulfils the industrial and human needs. Concerning greenhouse gas emissions and pollutants, and sustainability, there is a great demand to search for alternate feedstocks to produce alternate fuels at a low cost. The present work focuses on waste coconut and fish oil as potential inexpensive feedstock for biodiesel production. Two-stage transesterification processes for biodiesel production from hybrid oils mixed in a 1:1 volume ratio by employing solid nano-catalyst Magnesium Oxide (MgO). Response surface methodology (RSM) was used to analyze the effects of the physics of transesterification variables, such as methanol-to-oil molar ratio (M:O), MgO catalyst concentration (MgO CC), and reaction temperature (RT), on biodiesel yield, based on experimental data gathered in accordance with the matrices of central composite design (CCD). MgO CC showed the highest contribution, followed by M:O and RT, to maximize biodiesel yield. All interaction factors showed a significant effect except the M:O with RT. Grasshopper optimization algorithm (GOA) determined optimal conditions (M:O: 10.65; MgO CC: 1.977 wt.%; RT: 80 °C) based on empirical equations, resulting in maximum biodiesel yield conversion experimentally equal to 96.8%. The physical stability of the MgO nano-catalyst and reactivity up to 5 successive cycles can yield 91.5% biodiesel yield, demonstrating its reusability for sustainable biodiesel production at low cost. The optimized biodiesel yield showed better physicochemical properties (tested according to ASTM D6751-15C) to use practically in diesel engines.

**Keywords:** waste coconut oil; waste fish oil; transesterification process; nanocatalyst; response surface methodology; grasshopper optimization algorithm; biodiesel yield

## 1. Introduction

Fossil fuel (oil, natural gas, coal, etc.) depletion is a major threat to many countries' energy sectors and their dependent industries [1,2]. The use of combustible fossil fuels in industries and vehicles could result in abrupt changes in climatic conditions due to the accumulation of greenhouse gasses [3,4]. Human health is affected in many ways,

such as increased heat waves, floods and droughts, malnutrition, and vector-borne diseases (malaria, dengue, filariasis, onchocerciasis, Lyme, Chagas, African trypanosomiasis, etc.) [5,6]. Ever-increasing energy demand with technological advancement and stringent government regulations on environmental pollutants limit fossil fuel use, necessitating alternate fuel sources for IC and marine diesel engines [7,8]. Therefore, automobile industries are in an essential search to identify alternate fuel sources for diesel engines.

Biodiesel derived from triglycerides (i.e., waste cooking, vegetable oils, or animal fats) showed a promising substitute for conventional diesel fuel [9,10]. The transesterification process based on homogeneous or heterogeneous catalysts is commercially employed for biodiesel production [11]. Homogeneous alkali (NaOH and KOH) catalyzed transesterification reaction proved to be not only about 4000 times faster, but also available at low cost than acid catalysts [12,13]. Vegetable oils and animal fats are hydrophobic substances consisting of glycerol and fatty acids [14]. Higher content of unsaturated fatty acids possesses a greater technical advantage over vegetable oils [15]. However, biodiesel production based on vegetable oils is restricted due to the lack of cultivated land to grow enough plants and higher viscosity to use in diesel engines [16,17]. However, viscosity issues can be eliminated as subjected to the transesterification process [16]. India is the world's second-largest populated country, and reserving land for commercial usage (i.e., feedstock purely for biodiesel production) affects the shortage of land to grow food grains for their livelihood. Therefore, potential and low-cost feedstocks for biodiesel productions are to be researched that could meet the stringent need of energy requirements.

It is well known that 70% of the world's total earth crust is covered with water. India is encircled by three oceans—the Indian Ocean in the south, the Bay of Bengal in the east, and the Arabian Sea in the west—all of which produce a lot of fish. Fish heads, fins, skin, tails, liver, viscera, and other waste parts are used to make fish oils due to their high lipid content. [18,19]. In the economic context, biodiesel production from discarded fish parts is treated as less expensive. In addition, biodiesel production from fish oil could help to protect the environment; saturated and unsaturated fatty acids in fish oil possess high-cetane number, which increases the heating value in the combustion process [18,20–22]. The higher cetane number of biodiesel poses short ignition delay and advances the combustion timing [22]. The lesser emission characteristics (hydrocarbon, carbon monoxide, and smoke emission) was observed for fish oil derived biodiesel compared to diesel fuel [21,22]. The use of edible feedstock sources is restricted by national policy for food security, but waste coconut oil is a readily available alternative feedstock from homes, hotels, and restaurants, resulting in inexpensive production costs for biodiesel [23,24]. India, Indonesia, the Philippines, and Sri Lanka are the top countries contributing to global coconut production [25]. Coconut milk processing and manufacturing industries generate large tons of coconut meal waste, which are currently used as fertilizers in agriculture fields [26]. A potential feedstock for biodiesel is the waste produced by the coconut milk processing industry. Due to its accessibility, low free fatty acid content, improved lubricity, and similar flash point to diesel, coconut oil has significant advantages for the biodiesel production [27,28]. The use of waste coconut oil is estimated to convert 70% yield and achieve up to 96.5% methyl ester [29]. The factors that truly determine the yield of coconut oil are the age of the coconut, location of the plant, harvesting time, and extraction methods [26]. Ten million coconut farmers worldwide benefited with increase in income (from \$500 to \$5000 per year) as a result of using waste coconut oil for biodiesel conversion [26]. The waste coconut and fish oils can be considered as a viable replacement feedstock material for the production of biodiesel in light of the aforementioned discussions. Therefore, research investigations are to be carried out to test the practical usefulness of biodiesel in diesel engines.

The fish oil based on biodiesel showed better fuel properties (i.e., kinematic viscosity, calorific value, cetane number, flash point, peroxide value, and distillation temperature) than waste cooking oil [20]. Waste anchovy fish oils tested at full load direct compression ignition engine resulted in decreased performance values (i.e., engine torque of 4.14%, increased values of brake specific fuel consumption by 4.96%), and reduced emission char-

acteristics (carbon dioxide (CO<sub>2</sub>) value equal to 4.576%, carbon monoxide (CO) of 21.3%, and hydrocarbon (HC) of 33.42%) [21]. For the same engine test conditions, the oxygen, nitrogen oxides (NO<sub>x</sub>), and exhaust gas temperature increase to 9.63%, 29.37%, and 7.54%, respectively [21]. The common rail diesel engine parameters (injection timing and pressure) are studied to know their effect on emission (HC, NO<sub>x</sub>, CO) and performance (BSFC) characteristics of fish-oil biodiesel blends [30]. BSFC and NO<sub>x</sub> emissions increase with the reduced CO and HC values for all biodiesel (fish and waste cooking oils) blends [30,31]. The factors (temperature, molar ratio, catalyst concentration, stirring time, additives, and catalyst type) commonly affect biodiesel production [32]. The waste coconut-based biodiesel showed better engine performance and exhaust emissions than waste castor oils [33]. The above research confirmed that the waste coconut and fish oil-based biodiesel is best suited for diesel engines. However, research efforts are essential to maximizing the biodiesel yield (after converting a waste coconut and fish oil to biodiesel yield) subjected to optimization of the transesterification process.

Optimizing transesterification parameters reduced the biodiesel production costs [34], in addition to the low-cost feedstock selected (due to waste coconut oil and fish oil). Experiments examining the transesterification parameters influencing biodiesel production and cost are presented in Table 1. ANN model outperformed the CCD and BBD model in predicting the parameters that could result in the highest possible biodiesel yield conversion from WCO [35,36]. The ZnO/CaO nano-catalyst can be recovered and reused 3–4 times by using only a small quantity of catalyst (i.e., 1.66 wt.%), which converts oil to biodiesel yield [37]. Biodiesel yield increases with the increased concentration of CaO catalyst, microwave power, and reaction time [38]. CaO nanocatalyst exhibited 88.87% biodiesel conversion from refined bleached deodorized palm oil [39]. A higher reaction time of 96 h is required with the BCL catalyst for biodiesel conversion from coconut oil [40]. These results lead to a reduced production rate with increased production costs. Catalyst concentration resulted in dominating effect over methanol, reaction temperature, and reaction time in converting the biodiesel yield from waste fish oil [41,42]. In recent years, research work focused on mixing two or more oils, namely, edible and non-edible oils [43,44]; mix of thuma, linseed, palm, and karanj oil [45]; castor and soybean oil [46]; soybean oil and rapeseed oil [47]; and palm and cotton seed oil [48], for biodiesel conversion. Note that the OFAT approach requires more experimental trials than the design of experiments (CCD, BBD, and CCRD), but failed to locate global solutions might be due to neglecting the interaction factor effects [49]. CCRD should not be selected for experimental trials and analysis unless practical constraint dictates [50]. Desirability based design of experiments resulted in maximum of 91.5% biodiesel conversion from microalgae oil [51]. Furthermore, desirability approach resulted in better engine performances and reduces emission pollutants [52]. In the last two decades, many research attempts being made by conducting experimental and numerical types of research possessing low-cost feedstock for biodiesel production [53,54]. The following conclusions are drawn from the above-said literature: (a) transesterification factors (catalyst concentration and its type, reaction temperature, reaction time, and methanol-to-oil-molar ratio) are the major factors that require optimization for high-yield biodiesel; (b) although nano-catalyst resulted in better biodiesel yield with small quantity (in addition to recover-ability and reusability), not much research was being made to optimize parameters for higher biodiesel yield; (c) artificial intelligence tools (AI) gave better predictions than RSM, and there exists a significant scope to apply other AI tools for biodiesel yield-based process optimization; and (d) study of hybrid oils is in stringent demand due to the non-availability of individual oils in bulk quantity to meet the huge requirements for biodiesel production at a reduced cost.

**Table 1.** Biodiesel production via transesterification process utilizing various feedstocks.

| Feedstock Type     | Type of Catalyst               | Process Parameters  | Optimization     | Major Results | Ref. |
|--------------------|--------------------------------|---|------------------|---------------|------|
| WCO                | KOH                            | CC: 0.75–1.25 wt.%,<br>RT: 25–75 °C,<br>EOMR: 6–12                                | CCD and RSM, ANN | 96.7% yield   | [35] |
| WCO                | KOH                            | OEMR: 1:6–1:12,<br>Rt: 5–15 min,<br>MWP: 100–500 W                                | BBD and ANN      | 74.45% yield  | [36] |
| WCO                | ZnO/CuO oxide composite        | CC: 0.005–2.665 wt.%,<br>Rt: 15–235 min;<br>RT: 5–105 °C,<br>MOMR: 0–20           | CCRD and RSM     | 90.3% yield   | [37] |
| WCO                | CaO                            | CC: 1–3 wt.%,<br>MWP: 100–600 W;<br>Rt: 1–3.5 min;<br>RT: 5–110 °C,<br>MOMR: 0–20 | OFAT             | 33.84% yield  | [38] |
| WCO                | BCL                            | Rt: 96 h,<br>RT: 40 °C,<br>MOMR: 1:7  | OFAT             | 48% yield     | [40] |
| WFO (Sardine fish) | KOH                            | MQ: 20–30 vol.%,<br>CC: 0.75–1.75 wt.%,<br>Rt: 5–25 min                           | BBD              | 96.57% yield  | [41] |
| WFO                | KOH                            | CC: 0.5–1.5 wt.%,<br>RT: 30–60 °C,<br>EOMR: 7–13                                  | CCRD             | 96.41% yield  | [42] |
| WCO                | H <sub>2</sub> SO <sub>4</sub> | CC: 8–12 mL/L,<br>RT: 60–65 °C,<br>Rt: 100–120 min                                | OFAT             | NR            | [55] |
| WCO                | KOH                            | CC: 0.5–2.25 wt.%,<br>RT: 30–80 °C,<br>Rt: 30–70 min,<br>EOMR: 3–12               | OFAT             | 97.2% yield   | [56] |
| WFO                | NaOH and Na <sub>2</sub> HPO   | MOMR: 3.48–8.52,<br>Rt: 34–86 min,<br>RT: 43–77 °C                                | CCRD             | 94.6% yield   | [57] |

ANN: Artificial neural network; BBD: Box-Behnken Design; BCL: Burkholderia cepacia lipase; CC: Catalyst concentration; CCD: Central composite design; CCRD: Central composite rotatable design; EOMR: Ethanol to oil-molar ratio; KOH: potassium hydroxide; MOMR: Methanol to-oil molar ratio; Na<sub>2</sub>HPO: di-sodium orthophosphate; OEMR: Oil to-ethanol-molar ratio; OFAT: One-factor at-a-time; Rt: Reaction time; RSM: Response surface methodology; RT: Reaction temperature; WCO: Waste coconut oil; WFO: Waste fish oil; ZnO/CuO: Zinc oxide/copper oxide.

Many metaheuristic algorithms (particle swarm optimization, ant colony optimization, genetic algorithm, firefly algorithm, artificial bee colony optimization, grasshopper optimization, and so on) have proven their potential success in solving many optimization problems such as turning [58], drilling [59], biodiesel conversion [60], CNC turning [61], and abrasive water jet machining process [62]. Performance (solution accuracy and computation time) of the metaheuristic algorithms vary one with respect to another, and are truly dependent on tuning common and specific parameters of algorithms [59,60]. The metaheuristic algorithms are developed with common features, such as [63]: (a) search mechanisms employed with basic principles, namely velocity, force, and acceleration, and (b) mimic the social behavior of a group of animals. Grasshopper optimization algorithms (GOA) have proven their potential in solving many recent problems (engineering design, energy, image processing, and so on), namely, optimization [64,65]. However, few research

efforts are being made to optimize the biodiesel yield, viz., hybrid oil (waste fish oil and waste coconut oil) subjected to the transesterification process.

The present work attempted to use hybrid oils (i.e., waste coconut oil and waste fish oil) for biodiesel yield conversion at reduced production cost. The magnesium oxide MgO nanoparticles were used as a catalyst for biodiesel yield conversions from hybrid oil. Transesterification parameters were studied to examine the process analysis and determine the significant factors for high-yield biodiesel. CCD, the non-linear models developed for the transesterification process, could help to perform analysis, namely, factor (main and interaction) effects, surface plots (curvature effects), correlation coefficients, model adequacy, and prediction accuracy, such as regression equations. AI tools use CCD-derived regression equations for optimizing the transesterification parameters (MgO CC, M:O, reaction temperature) for higher biodiesel yield conversion. The reusability of solid catalyst was also examined. The optimized transesterification conditions are determined, namely, RSM based desirability function approach (RSM-DFA) and GOA, and the results are compared. The performance of GOA is tested for computation time and solution accuracy by conducting confirmation experiments. The optimized biodiesel yield sample was tested for physicochemical characteristics (viscosity, density, cetane number, heating value, and so on) that could examine the fuel properties suitable to use in diesel engines.

## 2. Materials and Methods

### 2.1. Sources of Waste Coconut Oil and Waste Fish Oil

The fish oil was purchased from the fish meal industry located near Ullal, Mangalore, Karnataka. The waste coconut oil was extracted by crushing the waste and unusable coconuts. The collected oils are filtered to remove the suspended solid particles. After filtration, heating the oils to remove the moisture content if any. Both the oils are mixing in 1:1 ratio by volume (50% Fish oil + 50% Waste coconut oil). The steps in preparing the hybrid oils are presented in Figure 1.

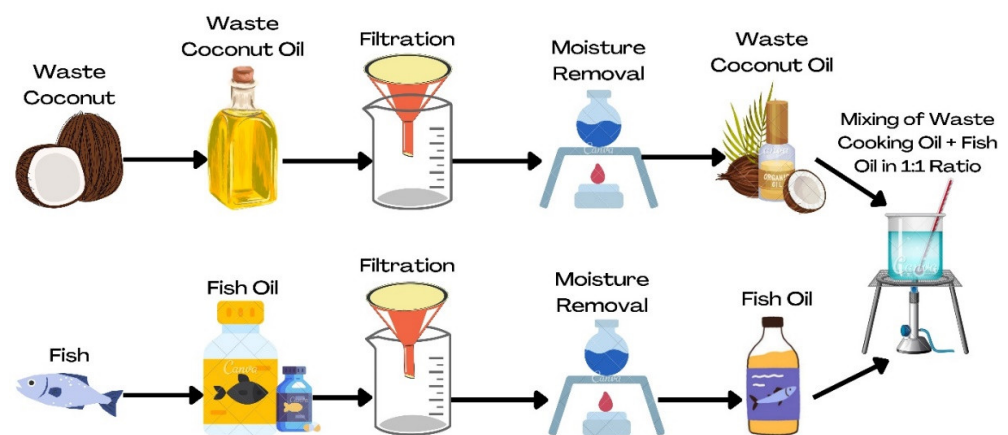


**Figure 1.** Steps in preparing hybrid oils.

### 2.2. Biodiesel Production Viz. Transesterification Process

Use of waste coconut and fish oils ensures low-cost feedstock and ensures greener environment, similar to palm fatty acid distillate using rice husk ash/nickel sulfate catalyst [66]. To prepare biodiesel, first, it is required to check the free fatty acid value, and based on that value, the transesterification process is to be selected. FFA level is determined by applying Isopropyl alcohol method. First, prepare the titration solution by dissolving 1 g of NaOH in 1 liter of distilled water. Take 1 mL of hybrid oil into the conical flask; add 10 mL of Isopropyl alcohol and four drops of phenolphthalein. Add the titration solution into the conical flask with continuous stirring of solution until it turns to faint pink color, and note down the titration value to calculate FFA. Single-stage transesterification can be

used if the FFA level is <4%, and two-stage transesterification can be used if the FFA level is >4%. The FFA computation of hybrid oil is done using Equation (1).

$$\begin{aligned} \text{FFA (\%)} &= \frac{28.2 \times \text{Normality of NaOH} \times \text{Titrate value}}{\text{Weight of oil}} \\ &= \frac{28.2 \times 0.1 \times 85}{10} = 24 \end{aligned} \quad (1)$$

FFA (%) of initial feedstock (before transesterification process) is 24.

### Acid Catalyzed Esterification

Hybrid oils containing excessively high free fatty acid content (% FFA > 4) has necessitated the use of a two-stage transesterification procedure. The low cost of methanol makes it the preferred alcohol for transesterification. In the first stage, 1 liter of hybrid oil, 6 mL of sulfuric acid ( $\text{H}_2\text{SO}_4$ ), and 150 mL of methanol were used. The acid catalyst undergoes quick catalyst reaction to convert high FFA to methyl ester. The above mixture is agitated in the 3-neck flask at 60 °C, and after 1½ hour, a dark layer will appear at the top of the oil. The mixture is poured into the separating funnel and allowed at least three hours to settle. The acid layer can be black at the top of the oil. Drain the oil at the bottom of the separating funnel into a 3-neck flask and collect the top layer. Take the sample obtained oil from a 3-neck flask, and the measured FFA level is reduced to less than 4%. The steps employed to transform hybrid oil (WCO +WFO) into biodiesel is presented in Figure 2.

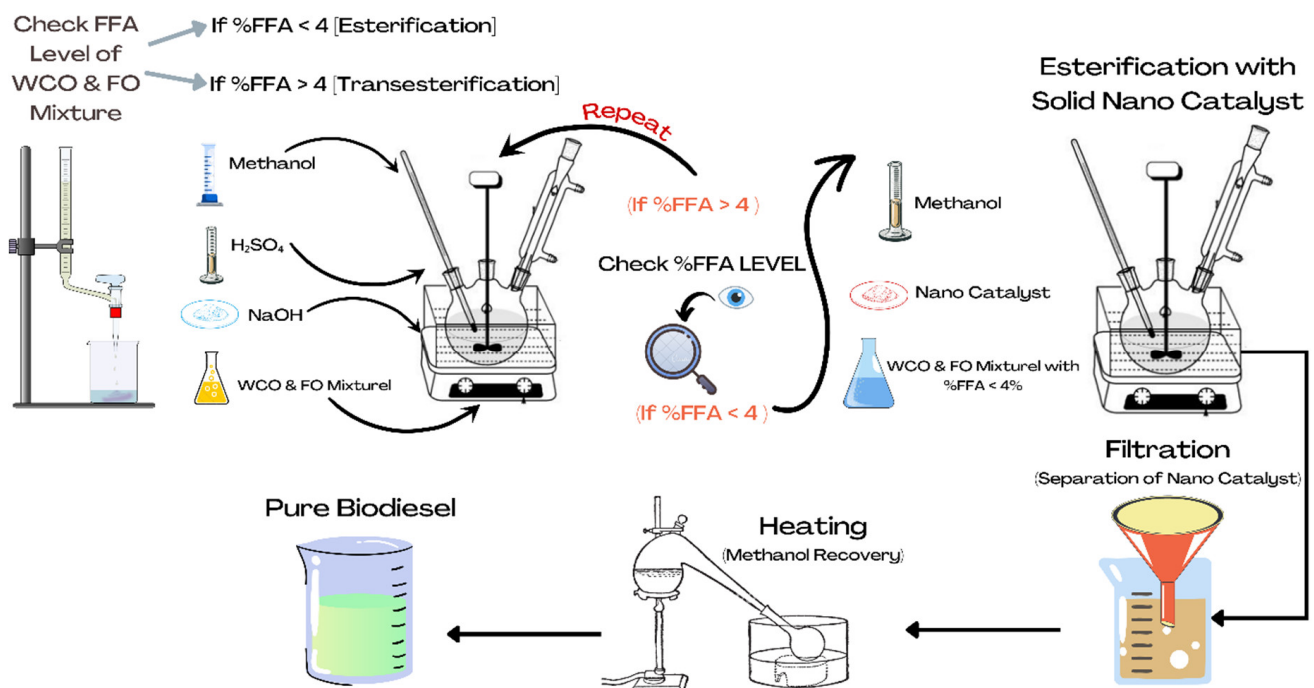
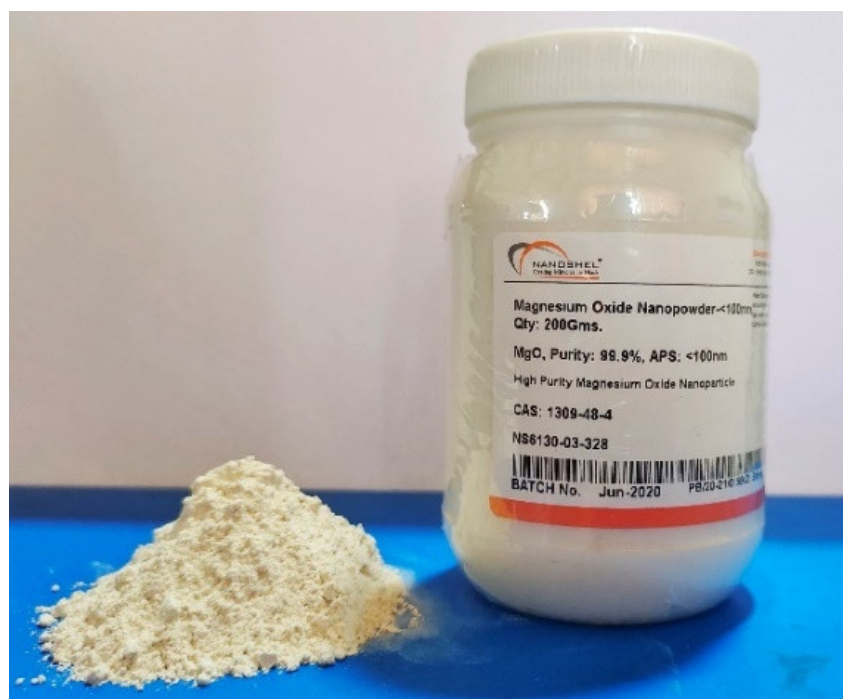


Figure 2. Steps in conversion of hybrid oils to biodiesel yield.

The second step involves transesterifying hybrid oil for two hours at 60 °C while utilizing a MgO nanocatalyst loaded at 2 % (*w/w*), methanol to oil molar ratio of 10:1 (*v/v*), and stirring rate of 300 rpm. After the two-stage transesterification reaction, the MgO nanocatalyst is filtered and can be reused, and methanol is recovered by heating (methanol will boil at 64 °C). The MgO nanocatalyst is less than 40 nm in size. It is purchased from Intelligent Materials Pvt. Ltd., Punjab, India. Magnesium Oxide (MgO) was used as a nanocatalyst because it is economical, environment friendly, and recyclable (refer to Figure 3). CaO catalyst has also shown reusability during transesterification process [67]. Thus, an acid pre-treatment step followed by a MgO nano-catalyzed step has been used to

convert hybrid oils samples into esters. The details of MgO nanoparticles are presented in Appendix A.



**Figure 3.** MgO nanocatalyst used for the present work.

### 2.3. Modeling and Analysis of Transesterification Process

Design of experiments is used to minimize the experimental runs in performing experiments and conducting statistical analysis. Face-centered central composite designs define the experimental matrix for three factors at respective three operating levels (refer to Table 2). To determine their impact on the conversion of biodiesel yield, three crucial transesterification variables (M:O, MgO CC, and RT) were investigated.

**Table 2.** Transesterification parameters and operating levels.

| Levels | Methanol to Oil Molar Ratio, A | Catalyst Concentration (wt.%), B | Reaction Temperature ( $^{\circ}$ C), C |
|--------|--------------------------------|----------------------------------|---|
| Low    | 3                              | 0.5                              | 50                                      |
| Medium | 8                              | 1.25                             | 65                                      |
| High   | 13                             | 2.0                              | 80                                      |

The experimental matrix represents transesterification variables as inputs defined viz. CCD is presented in Table 3. Three replicates for each experimental trial were considered, and the average values were used to analyze. RSM is a combination of mathematical and statistical techniques in which the variables are examined to detail the full understanding of a process (linear, square, and interaction factor effects). Coefficient of multiple correlation ( $R^2$  value) determines the model statistical adequacy, whose value is above 0.89 for the physical properties of biodiesel fuel derived from the blend of palm, olive and soybean oils [68]. Software (Design Expert version 11) defines the experimental plan and performs analysis and optimization.

**Table 3.** Face-centered central composite design for collecting input-output data.

| Run | A: Methanol to Oil Molar Ratio | B: Catalyst Concentration (Wt.%) | C: Reaction Temperature (°C) | Experimental Biodiesel Yield (%) | Predicted Biodiesel Yield (%) | Absolute Percent Deviation |
|-----|--------------------------------|----------------------------------|------------------------------|----------------------------------|-------------------------------|----------------------------|
| 1   | 03                             | 0.50                             | 50                           | 84.53                            | 83.86 ± 1.2                   | 0.793                      |
| 2   | 13                             | 2.00                             | 80                           | 94.45                            | 95.14 ± 0.3                   | 0.731                      |
| 3   | 08                             | 0.50                             | 65                           | 87.08                            | 87.52 ± 1.1                   | 0.505                      |
| 4   | 03                             | 2.00                             | 50                           | 81.93                            | 82.42 ± 0.8                   | 0.598                      |
| 5   | 08                             | 1.25                             | 65                           | 93.2                             | 93.28 ± 0.6                   | 0.086                      |
| 6   | 03                             | 0.50                             | 80                           | 81.55                            | 81.88 ± 0.8                   | 0.405                      |
| 7   | 08                             | 2.00                             | 65                           | 93.85                            | 93.29 ± 0.9                   | 0.597                      |
| 8   | 13                             | 0.50                             | 80                           | 82.62                            | 82.16 ± 1.3                   | 0.557                      |
| 9   | 13                             | 1.25                             | 65                           | 91.61                            | 91.31 ± 0.5                   | 0.327                      |
| 10  | 08                             | 1.25                             | 80                           | 93.45                            | 93.20 ± 0.3                   | 0.268                      |
| 11  | 08                             | 1.25                             | 65                           | 93.2                             | 93.28 ± 0.7                   | 0.086                      |
| 12  | 13                             | 0.50                             | 50                           | 82.60                            | 82.95 ± 0.9                   | 0.424                      |
| 13  | 08                             | 1.25                             | 65                           | 93.20                            | 93.28 ± 0.5                   | 0.086                      |
| 14  | 13                             | 2.00                             | 50                           | 89.63                            | 89.33 ± 0.6                   | 0.335                      |
| 15  | 03                             | 2.00                             | 80                           | 87.38                            | 87.05 ± 0.7                   | 0.378                      |
| 16  | 08                             | 1.25                             | 50                           | 91.16                            | 91.28 ± 0.4                   | 0.132                      |
| 17  | 03                             | 1.25                             | 65                           | 87.54                            | 87.72 ± 0.7                   | 0.206                      |

#### 2.4. Optimization of Transesterification Process

Experimental input–output data collected according to matrices of CCD were employed to derive an empirical regression equation. The coefficient of multiple correlations ( $R^2$  value) is used to evaluate the statistical adequacy of the regression equation obtained from the model. The  $R^2$  value close to 1 indicates the model is statistically significant. In recent years, artificial intelligence tools (GOA) have been used to search the optimal conditions with the help of objective functions (i.e., derived empirical regression equation viz. experimental input-output data) [59–62]. To carry out the optimization process and increase biodiesel yield, the GOA algorithm was applied. The MATLAB software platform is used to carry out the said task.

##### Grasshopper Optimization Algorithm

GOA showed promising results in solving many optimization problems [64,69]. GOA resulted in better performance might be due to the following reasons:

1. Grasshopper searched for multidimensional space with a large-step size in the early phases that could ensure identifying global solutions in an unseen area;
2. In the final phase, the grasshopper searched for solutions locally that could enhance the exploitation capabilities;
3. During the optimal search, the comfort zone factor balances the exploration and exploitation capabilities that assist grasshoppers in preventing premature convergence and locating global solutions [69];
4. Grasshoppers enhance the solutions from the initially generated random solutions over the progressive search as iteration progresses that could help to attain the global best fitness solutions.

GOA is a novel optimization technique wherein the algorithm is imitated by the social life of grasshopper insects (insects may be individual, or they form a maximum swarm group) in nature [70]. The grasshopper's life cycle is divided into two major phases: larval (slow with small step movement) and adulthood (large and unexpected movement). The grasshopper group shares the trait of having a common grouping behavior in both the nymph and adult stages. In either the nymph or adult phases, grasshoppers' primary

behaviors include foraging, target tracking, and team behaviors [70]. In the above phases, the grasshoppers search the food sources in both explorations (tends to move rapidly) and exploitation (tends to move slowly and locally) tendencies. A mathematical model is designed to simulate the said facts (swarming behavior of grasshoppers) as shown in Equation (2).

$$\underbrace{X_i}_{\text{Location or position of } i\text{th insect}} = \underbrace{S_i}_{\text{Social communication}} + \underbrace{G_i}_{\text{Gravity or pressure force on } i\text{th insect}} + \underbrace{A_i}_{\text{Wind advection}} \quad (2)$$

Equation (2) can be modified as follows,  $X_i = \text{rand}_1 S_i + \text{rand}_2 G_i + \text{rand}_3 A_i$ . Here, the terms  $\text{rand}_1$ ,  $\text{rand}_2$  and  $\text{rand}_3$  are random numbers whose value is between 0 and 1. Equation (2) is redefined with the help of Equations (3)–(5).

$$S_i = \sum_{\substack{j=1 \\ j \neq i}}^N s(|x_j - x_i|) \frac{x_j - x_i}{d_{ij}} \quad (3)$$

$$S_i = x_j - x_i / \underbrace{d_{ij}}_{\substack{\text{distance between} \\ \text{two grasshopper}}} \quad (4)$$

$$G_i = - \underbrace{g}_{\substack{\text{gravitational} \\ \text{constant}}} \underbrace{\hat{e}_g}_{\substack{\text{unity of vector} \\ \text{gravity}}} \quad (5)$$

$$A_i = \underbrace{u}_{\substack{\text{constant} \\ \text{drift}}} \underbrace{\hat{e}_w}_{\substack{\text{unity of vector} \\ \text{wind}}} \quad (5)$$

Term 's' represents the function that estimates the social attraction or repulsion forces and can be done by Equation (3).

$$\underbrace{S(r)}_{\substack{\text{comfortzone which is} \\ \text{either attractive or repulsive}}} = \underbrace{f}_{\substack{\text{amplitude} \\ \text{of attraction}}} e^{-r/l} - e^{-r} \quad (6)$$

In Equation (6), the term  $l$  represents the length scale, and  $r$  and  $f$  factors affect significantly the comfort zone, attraction, and repulsion. Then,  $f$  and  $l$  values are fixed to 0.5 and 1.5, respectively.  $N$  corresponds to the size of the swarm. The distance of insects is kept fixed equal to [1,4]. Equation (7) is constructed utilizing Equations (3)–(5).

$$X_i = \sum_{\substack{j=1 \\ j \neq i}}^N s(|x_j - x_i|) \frac{x_j - x_i}{d_{ij}} - g(\hat{e}_g) + u(\hat{e}_w) \quad (7)$$

The population is not converged to a predefined set goal because the grasshoppers could rapidly reach their comfort area. In such cases, the updated equation (Equation (8)) is used as follows,

$$X_i^d = c_1 \left( \sum_{\substack{j=1 \\ j \neq 1}}^N c_2 \left( \frac{UB_d - LB_d}{2} \right) s(|x_j^d - x_i^d|) \frac{(x_j^d - x_i^d)}{d_{ij}} + \hat{T}_d \right) \quad (8)$$

The term  $\hat{T}_d$  defines the best solutions reached so far. Term  $UB$  and  $LB$  refers to upper and lower bound,  $C_1$  decreases the movement of grasshopper and makes judgement by balancing two phases, such as exploration and exploitation search mechanism, and  $C_2$  decreases the comfort, attraction, and repulsion region between the grasshoppers. In Equation (8) the parameters  $C_1$  and  $C_2$  are treated as single parameter refers to  $C$ , which is a decreasing factor whose value can be estimated using Equation (9).

$$c = c_{\max} - \underbrace{l}_{\substack{\text{progress} \\ \text{of iteration}}} \frac{(c_{\max} - c_{\min})}{\underbrace{L}_{\substack{\text{upperbound} \\ \text{of iteration}}}} \quad (9)$$

Term  $C_{\max}$  be the maximum value, and  $C_{\min}$  be the minimum value of decreasing factor.

### 3. Results & Discussions

Experimental data (i.e., transesterification variables and biodiesel yield) collected based on the CCD matrix is examined for factor analysis (main, interaction, and curvature effects). The significance and model adequacy is tested, namely, analysis of variance. Empirical equations represent the output as biodiesel yield expressed mathematically as a function of inputs (transesterification variables). The derived regression equation is used as an objective function to locate the optimal conditions using GOA. The optimal conditions are tested experimentally and validated by the model. The reusability of nano-catalyst is also tested and confirmed their practical suitability. The test results of physicochemical properties corresponding to biodiesel yield are discussed.

#### 3.1. Data Collection

Transesterification experiments consider three variables (M:O, MgO CC, and RT) operating at three respective levels, according to the CCD matrix. The biodiesel yield measured at each experimental trial (repeated thrice) is treated to perform statistical analysis and derive regression equations by developing models (refer to Table 3). The average of three biodiesel yields corresponding to each experimental trial from 17 total experiments is found to vary with a maximum and minimum deviation equal to  $\pm 1.3$  and  $\pm 0.3$ , respectively.

#### 3.2. Main Effect Factor Analysis

Main effect factor analysis examines the individual factor contribution or effect (while other parameters are kept fixed to respective middle levels) on the biodiesel yield. Factor-wise analysis on output is explained below,

##### 3.2.1. Effect of Methanol-To-Oil Molar Ratio

Figure 4 explains the effect of the M:O ratio (analyzed between the ranges between 3–13) on biodiesel yield. During the M:O ratio analysis, factors such as MgO catalyst concentration and reaction temperature were fixed to 1.25 wt.% and 65 °C, respectively. An increased proportion of M:O up to the value equal to ~9 tends to increase the biodiesel

yield (93.2%) and, after that, decreases. At low values of M:O, the biodiesel yield is found to be equal to 87.71%. To induce a transesterification reaction, a minimum of three moles of methanol is essential to correspond to each mole of triglyceride [71]. Biodiesel yield can be increased with an excess proportion of methanol must be introduced into the crude oil, which could transform the equilibrium towards biodiesel production. After crossing the M:O equal to 9, a slight reduction in the biodiesel yield decreases slowly to a value equal to 91.31%. The results are attributed to the ratio corresponding to triglyceride to catalyst concentration (i.e., wt.%) being small, which increases the contact time of triglyceride as the catalyst surface increases. Furthermore, beyond the critical proportion of methanol to oil molar ratio, excess methanol transforms the triglycerides into monoglycerides. The difficulty in separating glycerol from biodiesel yield and the presence of glycerol in biodiesel shifts the equilibrium back to the left, causing decreased biodiesel yield [60]. Similar observations are reported for biodiesel conversion from waste cooking oil [71] and Niger seed oil [60].

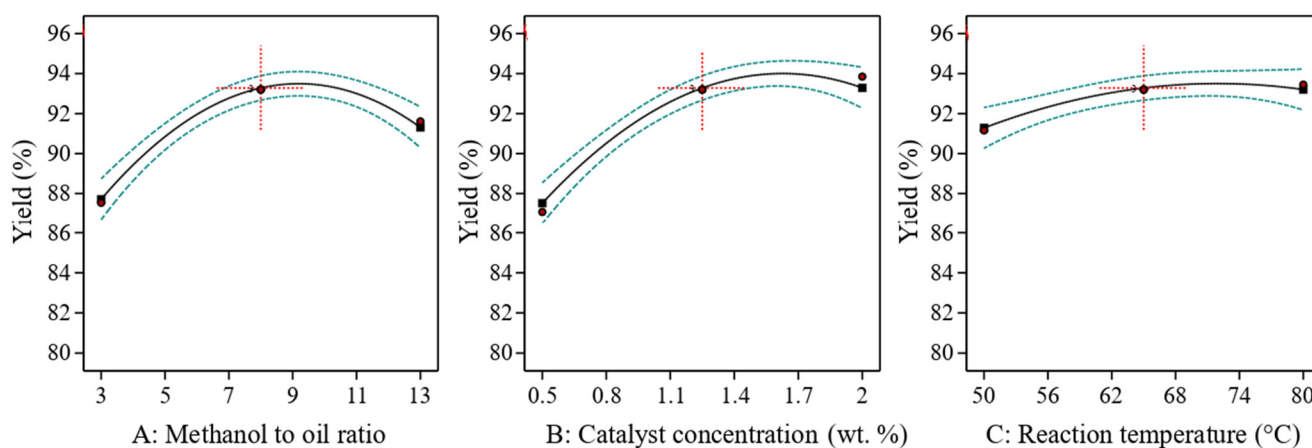


Figure 4. Main effect plot for biodiesel yield.

### 3.2.2. Effect of Catalyst Concentration

Figure 4 explain the influence of MgO CC (0.5 to 2 wt.%) on biodiesel yield. During the analysis of catalyst concentration, the M:O and RT kept fixed to 8 and 65 °C. Increased concentration of catalyst tends to improve the biodiesel yield 93.5% up to 1.5 wt.% and, thereafter, showed negligible decrease in biodiesel yield equal to 93.3% for 2 wt.%. The following reasons for attaining such results are [72,73]: (a) minimal concentration of catalyst is required to ensure complete transesterification reaction, wherein the initial reagents are adsorbed on the catalyst active center which tend to interact the formation of reaction product. (b) The total surface area improves with the increased concentration of catalyst led to maximum biodiesel conversion. The negative impact on biodiesel conversion when the catalyst concentration increases beyond the critical value might be due to following reasons [74–76]: (a) the reaction mixture tends to become more viscous and often find difficulty in mixing liquid reactants with solid nanocatalyst. (b) Few percent of catalyst remain non-reactive due to mass transfer resistance and reaction products absorbed on the catalyst surfaces.

### 3.2.3. Effect of Reaction Temperature

The influence of reaction temperature (varied in the ranges of 50 to 80 °C) on the performance of biodiesel yield is explained in Figure 4. Reaction temperature analysis was carried out after keeping the M:O and MgO CC fixed equal to 8 and 1.25 wt.%. Following an increase in reaction temperature up to ~70 °C, the biodiesel yield also increases from 91.28% to 93.3%, and later showed negligible change in biodiesel yield (93.4%) when the reaction temperature attained a higher value equal to 80 °C. The biodiesel yield decreases after attaining the optimal temperature might be due to the following reasons [71,76]: higher

vaporization of methanol, the undesirable reaction of feedstock, and formation of reaction products (i.e., involvement of other MgO surface active sites), and bubbles formation reduces the interface of oil and methanol, which causes an undesirable effect in biodiesel conversion. The reaction temperature is treated as a critical parameter (although their effect on biodiesel yield is negligibly small compared to M:O and MgO CC) in minimizing the production cost of biodiesel.

### 3.3. Interaction Factor Analysis: Surface Plot

Figure 5a–c showed the surface plots (3-Dimensional) that could explain the effect of 2-term factors interaction between M:O, MgO CC, and RT on biodiesel yield.

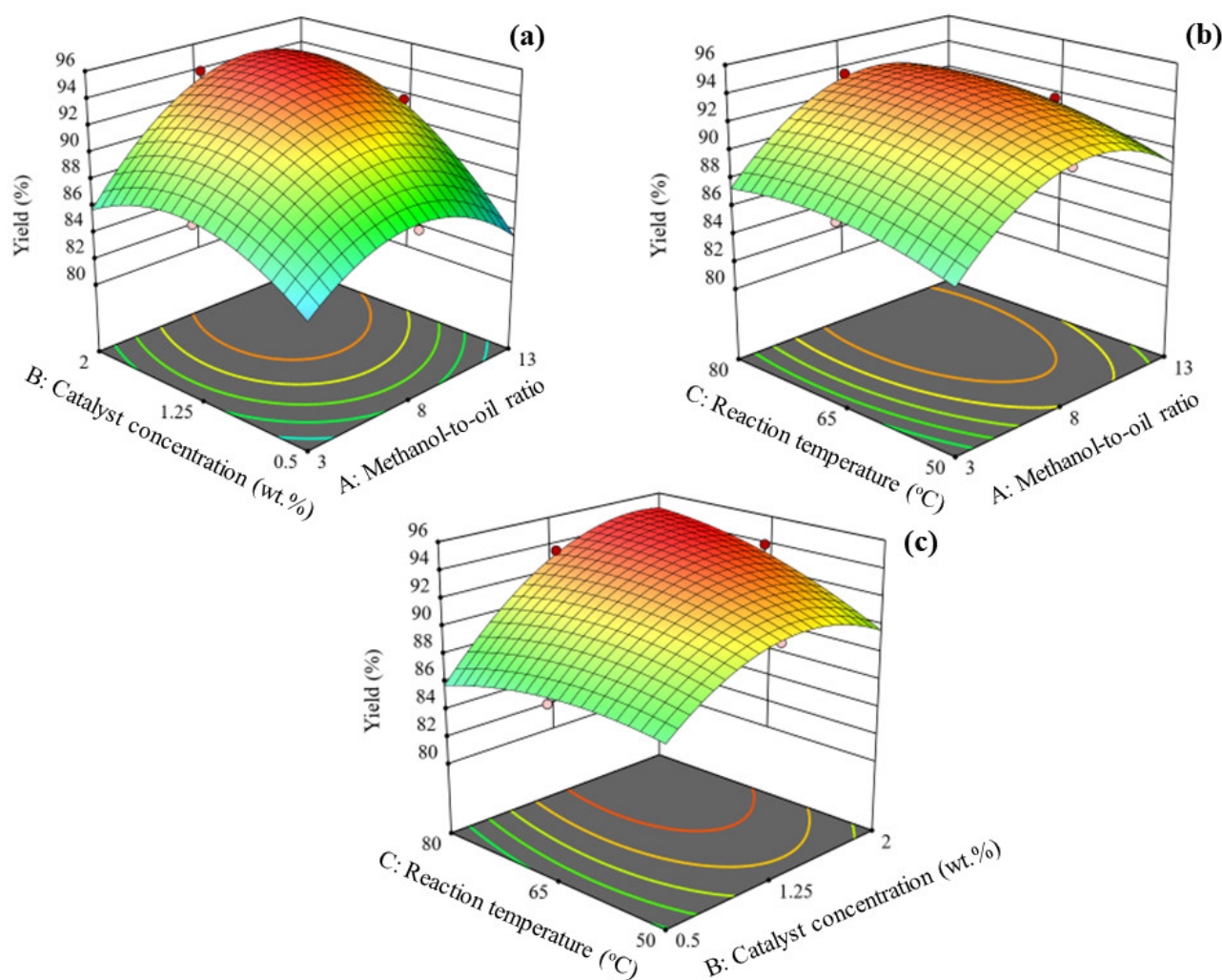


**Figure 5.** Surface plots of transesterification factors (M:O, MgO CC, RT) vs. yield: (a) M:O and MgO CC, (b) M:O and RT, and (c) MgO CC and RT.

1. The biodiesel yield tends to improve with an increase in catalyst concentration and methanol-to-oil ratio up to the middle levels (refer to Figure 5a). The reaction temperature was kept fixed to 65 °C (the middle value of the operating range of RT) during the analysis. Catalyst concentration showed higher raise in biodiesel yield compared to the methanol-to-oil molar ratio. Increased concentration of MgO nanocatalyst increases the contact and availability of basic sites between catalyst and reactants, causing higher yield [77]. As the methanol-to-oil molar ratio was increased, the viscosity of the reaction mixture due to agitation involved in the transesterification process decreased (equilibrium shift towards the conversion side), resulting in increased biodiesel yield [24]. The combination of the highest catalyst concentration and

methanol-to-oil ratio showed reduced biodiesel yield. The highest catalyst concentration with methanol to oil molar ratio could result in soap formation due to incomplete reaction. It is often difficult to separate the glycerol and biodiesel, resulting in reduced biodiesel yield [78].

2. Figure 5b explains the effect of reaction temperature with methanol-to-oil molar ratio when the catalyst concentration of MgO is fixed to 1.25 wt.%. An increase in methanol-to-oil molar ratio up to ~10 increases the biodiesel yield. Beyond the critical value (i.e., after ~10), the conversion of biodiesel yield is reduced. The reduced biodiesel yield is beyond the required amount of methanol which tends to accumulate on the catalyst surface, reducing the reaction (due to the reduction of active sites) mixture and process efficacy in the conversion of higher yield [79]. Beyond the critical reaction temperature, the methanol transforming from the liquid phase to gas results in poor interaction between methanol oil and gases, decreasing biodiesel yield [80]. The resulted surface plot clearly shows that reaction temperature is less affected than the methanol-to-oil molar ratio towards converting oil to biodiesel yield.
3. Figure 5c explains the interaction factor effects of reaction temperature and catalyst concentration tested for a fixed methanol-to-oil molar ratio equal to 8. The effect is seen to have a similar trend with more pronounced than the factors interaction of methanol-to-oil molar ratio and reaction temperature. The catalyst concentration up to the middle value of 1.25 wt.% increases the biodiesel yield and decreases later. Higher catalyst particles tend to accumulate and form a bulk mass, reducing the catalyst's active surface area and increasing the mixture's viscosity [81]. The effect of the reaction temperature is negligibly small compared to catalyst concentration. Increased values of reaction temperature decrease the biodiesel yield probably due to increased miscibility caused by a collision between the species; methanol vaporization ensures decreased availability of methanol in the reaction mixture. Similar observations are reported in the published literature [82].

### 3.4. Mathematical Regression Equation

The CCD matrix-based transesterification experiments are carried out to derive empirical equations wherein biodiesel yield (output or dependent variable) is expressed as a function of transesterification variables (inputs or independent variable). Table 4 presents the details of models fitted (linear, linear + square + interaction, linear + interaction) based on experimental input-output data.

**Table 4.** Fitted models correspond to experimental input-output data.

| Model                         | Regression Equation   | Regression Coefficient                                    |
|-------------------------------|---|---|
| Linear                        | Yield = 76.92 + 0.36 A + 3.848 B + 0.064 C  | R <sup>2</sup> = 0.3542, and Adj. R <sup>2</sup> = 0.2052 |
| Linear + Interaction          | Yield = 96.12448 – 0.5484A – 9.875B – 0.1514C + 0.521AB + 0.004 AC + 0.147 AC   | R <sup>2</sup> = 0.5049, and Adj. R <sup>2</sup> = 0.2078 |
| Linear + Interaction + Square | Yield = 63.54662 + 1.86215 A + 2.90935 B + 0.447504 C + 0.521 AB + 0.00395 AC + 0.147 BC – 0.150659 A <sup>2</sup> – 5.11374 B <sup>2</sup> – 0.004607 C <sup>2</sup> | R <sup>2</sup> = 0.9869, and Adj. R <sup>2</sup> = 0.9737 |

RSM is applied to derive regression equations presented in Table 4. Three models have been developed from experimental input-output data. The model adequacies are evaluated based on the coefficient of determination. The models evaluate the input variables based on the preset confidence level (i.e., *p*-value = 95%). The model with all terms (significant and insignificant) representing input variables is estimated with an R<sup>2</sup> value. The exclusion of insignificant terms (i.e., *p*-value > 0.05) from the models is referred to as the Adjusted R<sup>2</sup> value. The best fit model always corresponds to the R<sup>2</sup> value close to 1. The best fit model is obtained with full quadratic terms (linear + interaction + square), producing a better R<sup>2</sup> value and Adj. R<sup>2</sup> values equal to 0.9869 and 0.9737, respectively. The full quadratic model showed a better correlation between the biodiesel yield and transesterification

variables. Therefore, regression equations corresponding to full quadratic terms were used to predict the biodiesel yield for all experimental trials (refer to Equation (10) and Table 3). The regression equation corresponds to full quadratic terms representing biodiesel yield expressed as a mathematical function of transesterification variables is presented below,

$$\text{Yield (\%)} = +63.54662 + \underbrace{+1.86215 A + 2.90935 B + 0.447504 C}_{\text{Main factors}} + \underbrace{+0.521 AB + 0.00395 AC + 0.147 BC}_{\text{Interaction factors}} - \underbrace{0.150659 A^2 - 5.11374 B^2 - 0.004607 C^2}_{\text{Square factors}} \quad (10)$$

To understand the transesterification process, examining all the transesterification variables that influence biodiesel yield is essential. The model (all terms: linear, square, and interaction) is statistically significant as their  $p$ -value is found to be less than 0.05 (refer to Table 5). All the main effect parameters (linear: M:O, MgO CC, and RT) were significant because their  $p$ -value was less than 0.05. Note that the MgO CC showed a maximum effect than M:O and RT and is in good agreement with the effects of variations of transesterification variables on biodiesel yield (refer to Figures 4 and 5). The square terms of all transesterification variables are less than 0.05  $p$ -values, indicating that all variables have a nonlinear relationship with biodiesel yield (refer to Figure 5). The F and  $p$ -values of linear, squared, and interaction terms with their effects were statistically significant ( $p$ -value < 0.05). Only the interaction term (M:O and RT) was found statistically insignificant among the full quadratic model terms. The inclusion of insignificant interaction terms in the model-derived empirical equation does not explain the variability in response (biodiesel yield) subjected to different transesterification variables. However, insignificant terms (methanol-to-oil ratio  $\times$  reaction temperature) need not be excluded from the derived empirical regression equation because they not only present imprecise input-output relationships, but also reduces the prediction accuracies. Therefore, predictions are to be made with the inclusion of all terms for better prediction accuracies.

**Table 5.** Analysis of variance for biodiesel yield.

| Source         | Sum of Squares | DF | Mean Square | F-Value | $p$ -Value |
|----------------|----------------|----|-------------|---------|------------|
| Model          | 349.91         | 9  | 38.88       | 107.18  | <0.0001    |
| A: M:O         | 32.33          | 1  | 32.33       | 89.12   | <0.0001    |
| B: MgO CC      | 83.29          | 1  | 83.29       | 229.62  | <0.0001    |
| C: RT          | 9.22           | 1  | 9.22        | 25.41   | 0.0015     |
| AB             | 30.54          | 1  | 30.54       | 84.19   | <0.0001    |
| AC             | 0.7021         | 1  | 0.7021      | 1.94    | 0.2068     |
| BC             | 21.88          | 1  | 21.88       | 60.32   | 0.0001     |
| A <sup>2</sup> | 38.01          | 1  | 38.01       | 104.79  | <0.0001    |
| B <sup>2</sup> | 22.17          | 1  | 22.17       | 61.12   | 0.0001     |
| C <sup>2</sup> | 2.88           | 1  | 2.88        | 7.94    | 0.0259     |
| Residual       | 2.54           | 7  | 0.3627      |         |            |
| Lack of Fit    | 2.54           | 5  | 0.5078      |         |            |
| Pure Error     | 0.0000         | 2  | 0.0000      |         |            |
| Cor Total      | 352.45         | 16 |             |         |            |

DF: Degrees of freedom; F-value: Fisher value;  $p$ -value: Preset confidence level.

The model predicted, namely, full quadratic regression equation (i.e., Equation (10)), is tested for prediction accuracies and compared with experimental values (different settings of transesterification variables), resulting in best-fit data points close to the trend line (refer to Figure 6). The average absolute percent deviation in prediction considering all 17 experiments are found to be 0.3829. The full quadratic regression equation predicts the biodiesel yield accurately (with less percent error). Therefore, Equation (10) can be applied to search with different sets of transesterification variables to maximize biodiesel yield.

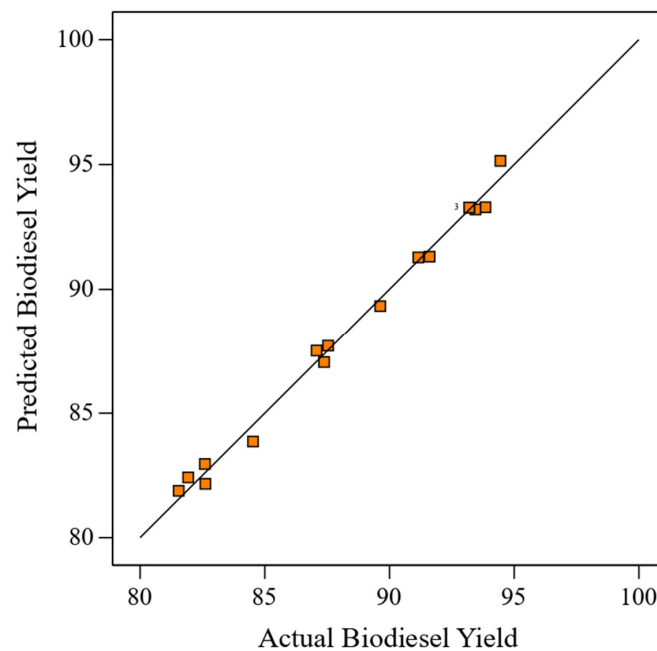


**Figure 6.** Predicted versus actual or experimental biodiesel yield.

### 3.5. Summary Results of GOA and RSM-DFA

RSM-DFA and GOA methods are applied to maximize the biodiesel yield by varying transesterification variables (M:O, MgO CC, and RT) of their respective operating range. The optimization problem is formulated as follows:

The objective function employed to determine the maximum yield is presented in Equation (11).

Maximize

$$\begin{aligned} \text{Yield (\%)} = & +63.54662 + 1.86215 A + 2.90935 B + 0.447504 C + 0.521AB + 0.00395AC \\ & + 0.147BC - 0.150659A^2 - 5.11374B^2 - 0.004607C^2 \end{aligned} \quad (11)$$

The RSM-DFA and GOA conduct optimal search correspond to upper and lower bounds of transesterification variables that maximizes the biodiesel yield is presented below,

Subjected to

$$\begin{aligned} \text{Methanol – to – oil – molar ratio} & = 3 \leq A \leq 13, \\ \text{MgO catalyst concentration} & = 0.5 \leq B \leq 2.0, \\ \text{Reaction temperature} & = 50 \leq C \leq 80 \end{aligned}$$

The RSM-DFA and GOA determine the optimized transesterification conditions that maximizes the biodiesel yield is presented in Table 6. Note that GOA determined optimized transesterification conditions resulted in maximized biodiesel yield equal to 95.95%, compared to RSM-DFA of 94.96%. GOA outperformed DFA might be due to the following reasons: (a) response surface (output function) behaves either unimodal (i.e., either maximize or minimize) or multimodal (both maximized and minimized) in multidimension search space of input variables [83]. (b) DFA employs deterministic search procedure with specific rules that move solution one with respect to other in a single direction resulted in many sub-optimal solutions [84]. (c) GOA is stochastic in nature and conduct search with set of probabilistic transition rules in multi-dimension search space at many spatial locations simultaneously. (d) The response surface (biodiesel yield) of the present work behaves multi-modal in nature (with variations in transesterification variables) and results in more than one optimal solution. (e) GOA solve multimodal problem more effectively than RSM-DFA.

**Table 6.** Optimization of transesterification parameters viz. GOA and RSM.

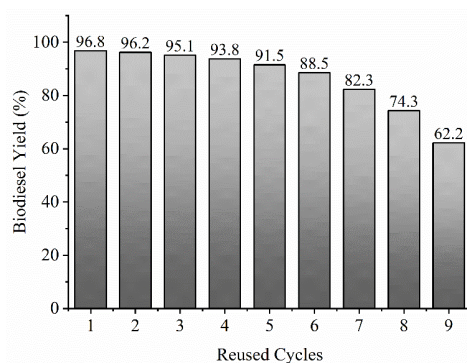
| Optimization Method | Algorithm Specific Parameters   | Fitness Value (Yield %) | Computation Time (Seconds) | Transesterification Condition                 |
|---------------------|---|-------------------------|----------------------------|---|
| GOA                 | $C_{\max}$ : 1<br>$C_{\min}$ : 0.00003<br>Population size: 40<br>Maximum iteration: 100 | 95.95%                  | 30                         | M:O = 10.65; CC = 1.977 wt.%;<br>RT = 80 °C   |
| RSM-DFA             | NA  | 94.96%                  | NA                         | M:O = 11.19; CC = 1.72 wt.%;<br>RT = 69.92 °C |

NA: Not applicable; RSM-DFA: Response surface methodology-based desirability function approach.

The GOA performances were examined based on solution accuracy. The solution accuracy is reliant on the appropriate tuning of parameters (algorithm-specific:  $C_{\max}$  and  $C_{\min}$ ; and common: population size and maximum iteration) [85]. The parameters are tuned after conducting successive trials and the best solution in terms of fitness value (i.e., maximized value of biodiesel yield) is determined. The optimal transesterification conditions that maximize biodiesel yield correspond to tuned algorithm parameters are presented in Table 6. Experiments were conducted correspond to optimal transesterification conditions (M:O: 10.65, MgO CC: 2 wt.%, and RT: 80 °C) to confirm the practical utility to apply in industries. The experiments resulted with the maximum biodiesel yield (average values of three times repeated experiments correspond to optimal transesterification condition) equal to 96.8%. The time elapsed to locate the optimal transesterification conditions tested on MATLAB software installed in personal computer (configuration: 4 GB RAM; Intel Core i3 processor, 1.2 GHz CPU) is 30 s. Less computation time with better solution accuracy explain the efficacy of GOA, and the results are beneficial (systematic method ensures no need of expert's recommendation and their dependency, limits the trial-and-error experiments, reduced material waste and time, and can be employed in online monitoring for maximum biodiesel conversion from hybrid oil) to industries for biodiesel production at low cost. Lowering the biodiesel production cost is essential to industries for commercialization [86].

### 3.6. Reusability of MgO Nanocatalyst

The cost of biodiesel relies on feedstock, energy consumption, labor, catalyst, etc. The results indicated that ~70–80% of the total production cost of biodiesel is accountable to feedstock [87–89]. Reusability of solid nanocatalyst could significantly reduce the high cost of MgO nanocatalyst. Experiments are carried out for nine successive cycles at an optimal transesterification condition (M:O: 10.65, MgO CC: 2 wt.%, and RT: 80 °C) determined using GOA. After ensuring a complete cycle of transesterification reaction during biodiesel conversion, the MgO catalyst was recovered or separated from the liquid (biodiesel yield) product subjected to filtration, followed by methanol wash. Later the MgO nanocatalyst was dried in an oven subjected to 100 °C and reused for the next cycle. Figure 7 shows the results of biodiesel yield conversions of nine cycles. The result showed that the conversion rate of biodiesel yield from hybrid (waste coconut and fish oil) oil decreases from 96.81% for the fresh or first used catalyst to 60.43% for the ninth reuse.

**Figure 7.** Reusability study of MgO nanocatalyst.

The drop in biodiesel conversion from hybrid oil (waste coconut oil + waste fish oil) is attributed to the following reasons [24,82,90]: (a) partial leaching (i.e., the solubility of Mg in methanol phase) of Mg in reaction mixture over successful cycles; (b) fresh catalyst show crystallinity with definite edges and shapes (refer to Figure 8a), whereas agglomeration of the catalyst after transesterification reaction resulted in deactivation of the catalyst (refer to Figure 8b); (c) block of the catalyst over sites by-products formed (biodiesel yield) during the reaction lead to catalytic poisoning (refer to Figure 8b); and (d) after each cycle, the catalyst recovered loses the crystallinity, which results in loss of catalytic activity.

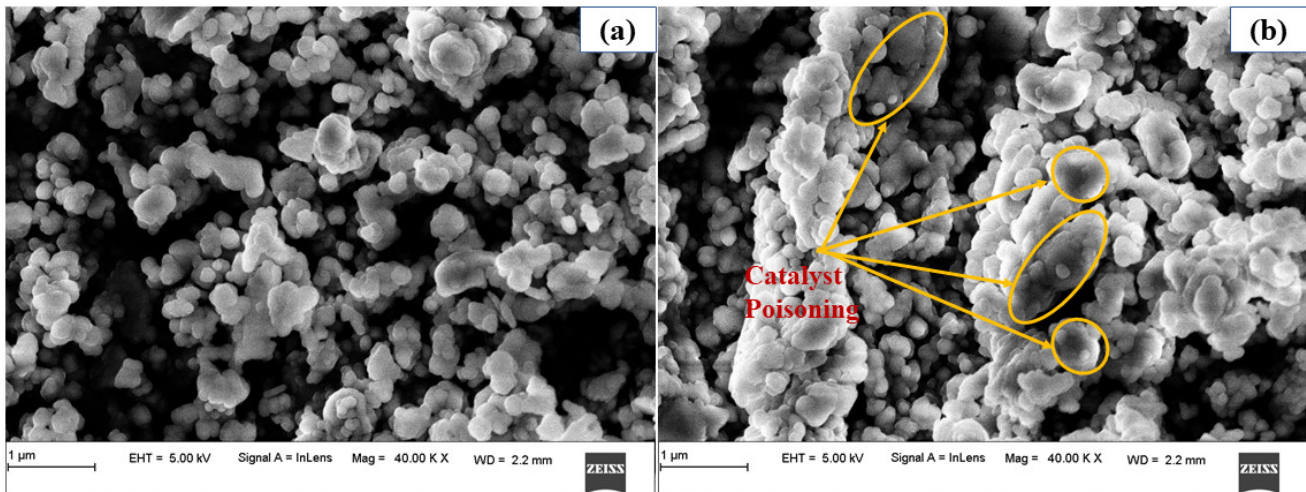


**Figure 8.** SEM images of MgO: (a) MgO before transesterification and (b) MgO after transesterification.

### 3.7. Physicochemical Properties Evaluation: Biodiesel Yield, Hybrid Oil, WCO, WFO

The biodiesel yield obtained according to the optimized transesterification conditions is subjected to physicochemical fuel properties examination to know their practical usefulness in diesel engines. The testing of fuel properties is done according to ASTM standards. All fuels (WCO, WFO, WCO + WFO, diesel, and biodiesel yield) and their properties (considering average values of three replicate experimental fuel properties) are determined and compared with standards designated for biodiesel to use in diesel engines. Specific gravity affects the fuel injection system. Transesterification of biodiesel yield resulted in the specific gravity within the acceptable ranges ( $0.87$  to  $0.89$   $\text{kg}/\text{m}^3$ ) as per biodiesel standard. Note that WFO, WCO, and hybrid oil possess specific gravity  $> 0.91$   $\text{kg}/\text{m}^3$ , and after transesterification reaction of hybrid oil reduces the biodiesel yield to  $0.88$   $\text{kg}/\text{m}^3$ . The oils (WFO, WCO, and WFO + WCO) exhibit higher viscosity and density: decide the mass of fuel flowing into the engine, flash, and fire point with low calorific value compared to diesel (refer to Table 7). Using the above fuels without transesterification affects the fuel injection system, deposits in exhaust ducts, and increased wear of parts directly linked to oils [91]. High flash and fire points of biodiesel yield are often advantages in handling, storage, and transportation and ensure non-hazardous fuel [92]. The calorific or heating value of biodiesel yield is  $40.8$   $\text{MJ}/\text{Kg}$ , which is comparatively lesser than the  $43.8$   $\text{MJ}/\text{Kg}$  for diesel fuel. The presence of oxygen content lowers the calorific value of biodiesel yield [93]. The ignition time delay and combustion quality are affected by the cetane number. Higher cetane number of biodiesel yield poses advantages, such as reduced noise, less emission, better fuel combustion, and engine output [94,95]. The cloud point and pour point values of biodiesel are within the permissible limit of biodiesel standards for diesel engines. All the major biodiesel fuel properties are within the permissible limit and comply with diesel fuel.

**Table 7.** Physicochemical properties of WFO, WCO, hybrid oil (WFO + WCO), diesel, and biodiesel.

| Properties   | WFO   | WCO   | WFO + WCO | Biodiesel | Diesel | Test Standard: ASTM D6751-15C |
|--|-------|-------|-----------|-----------|--------|-------------------------------|
| Specific gravity, kg/m <sup>3</sup>                    | 0.91  | 0.93  | 0.92      | 0.88      | 0.87   | 0.85 to 0.9                   |
| Kinematic Viscosity at 40 °C, cSt (mm <sup>2</sup> /s) | 24.20 | 28.42 | 26.43     | 4.67      | 4.1    | 1.4 to 1.6                    |
| Density, kg/m <sup>3</sup>                             | 893   | 923   | 905       | 840       | 800    | 880 max.                      |
| Flash Point, °C  | 224   | 266   | 253       | 131       | 58     | 100 min.                      |
| Fire Point, °C   | 233   | 275   | 237       | 146       | 64     | -                             |
| Calorific Value, MJ/kg                                 | 36.2  | 37.4  | 36.9      | 40.8      | 43.8   | -                             |
| Cloud Point, °C  | 19    | 5     | 11        | 6         | −7     | −3 to 12                      |
| Cetane index   | 56    | 52    | 54.3      | 63.7      | 50.3   | 47 min.                       |
| Pour Point, °C   | 6     | 3     | 5         | 4         | −8     | −15 to 10                     |

#### 4. Conclusions

The cost-effective approach (feedstock: WCO, WFO; catalyst: reusable MgO nanocatalyst; transesterification process; experimental methodology: CCD; optimization: GOA) is employed to ensure sustainability in biodiesel production. The following conclusions are drawn,

- Using waste fish oil and coconut oil reduces feedstock cost (feedstock alone constitutes ~80% of total biodiesel conversion cost) and biodiesel conversion cost. CCD limits the large-scale experiments (reduces the material, time, equipment, energy, labor, and so on) to detail the process insights. GOA conducts optimal search (namely, regression equations derived with experimental data) to obtain global values (biodiesel yield) at reduced computation time of 30 s, without needing practical experiments;
- CCD-based experimental matrix was planned to study transesterification variables (M:O, MgO nanocatalyst, and RT) on biodiesel yield. All three linear (M:O, MgO nanocatalyst, and RT) parameters are found to make a significant contribution to biodiesel conversion. MgO CC contributions are more, followed by M:O and RT. The square terms of all three transesterification variables were significant, clearly defining non-linear relation with the biodiesel yield. All interaction terms (excluding M:O × RT) were found significant;
- The full quadratic model (linear + interaction + square terms) produces the best fit with an R<sup>2</sup> value of 0.9869, resulting in prediction accuracy of 0.3829. The better prediction ensures model-derived empirical regression equations are statistically adequate and best suited for searching for optimal transesterification conditions that maximize biodiesel yield;
- GOA tuned parameters (C<sub>max</sub>: 1; C<sub>min</sub>: 0.00003; population size: 40; and maximum iteration: 100) resulted in maximum biodiesel conversion of 96.8% subjected to an optimal transesterification (M:O: 10.65, MgO CC: 2 wt.%, and RT: 80 °C) conditions;
- The MgO catalyst was recycled nine times to examine the stability and reusability under the optimal transesterification reaction conditions. The MgO nanocatalyst reused up to five cycles showed a negligible reduction (stable) in biodiesel yield from 96.8% to 91.5%, later reduced to 62.2% after nine cycles. Loss of crystallinity, agglomeration, and catalytic poisoning resulted in catalyst deactivation, and thereby reducing biodiesel conversion. However, stability and reusability of catalyst up to five cycles without catalyst deactivation ensures reduction of the catalyst cost in turn biodiesel production cost;
- The physicochemical properties of biodiesel fuel (conversion from hybrid oil: waste fish oil + waste coconut oil) are within the acceptable limit of biodiesel standard and are suitable to use in diesel engines.

**Author Contributions:** Conceptualization, I.Y.D., L.M.M. and P.S.; methodology, A.B.S., M.P.G.C. and C.P.; software, M.P.G.C., I.Y.D., A.B.S. and P.S.; validation, I.Y.D., L.M.M., C.P. and P.S.; formal analysis, I.Y.D., L.M.M., A.B.S. and M.P.G.C.; investigation, I.Y.D., L.M.M., A.B.S. and C.P.; resources, I.Y.D., P.S. and C.P.; writing—original draft preparation, M.P.G.C., I.Y.D., A.B.S. and P.S.; writing—review and editing, I.Y.D., L.M.M., P.S., A.B.S., M.P.G.C. and C.P. All authors have read and agreed to the published version of the manuscript.

**Funding:** The authors are pleased to acknowledge that the work reported in this paper was supported by Visveswaraya Technological University, Belagavi, related to Competitive Research Fund (Reference: VTU/TEQIP 3/2019/321) under TEQIP Program.

**Institutional Review Board Statement:** Not applicable.

**Informed Consent Statement:** Not applicable.

**Data Availability Statement:** Not applicable.

**Conflicts of Interest:** The authors declare no conflict of interest.

### Appendix A. Details of Specification of MgO Nano Powder Used as a Catalyst

|                   |                                |
|-------------------|--------------------------------|
| Form              | Powder                         |
| Color             | White                          |
| Odor              | No Odor                        |
| Purity            | 99.9%                          |
| APS               | <100 nm                        |
| Molecular Formula | MgO                            |
| Molecular Weight  | 40.304 g/mol                   |
| Density           | 3.58 g/cm <sup>3</sup>         |
| Melting Point     | 2852 °C                        |
| Boiling Point     | 3600 °C                        |
| Stability         | Completely Stable              |
| Solubility        | Insoluble in Water and Ethanol |

### References

1. IEA. *Net Zero by 2050: A Roadmap for the Global Energy Sector*; OECD Publishing: Paris, France, 2021. [\[CrossRef\]](#)
2. Holechek, J.L.; Geli, H.M.; Sawalhah, M.N.; Valdez, R. A Global Assessment: Can Renewable Energy Replace Fossil Fuels by 2050? *Sustainability* **2022**, *14*, 4792. [\[CrossRef\]](#)
3. Shen, M.; Huang, W.; Chen, M.; Song, B.; Zeng, G.; Zhang, Y. (Micro) plastic crisis: Un-ignorable contribution to global greenhouse gas emissions and climate change. *J. Clean. Prod.* **2020**, *254*, 120138. [\[CrossRef\]](#)
4. Khalili, S.; Rantanen, E.; Bogdanov, D.; Breyer, C. Global transportation demand development with impacts on the energy demand and greenhouse gas emissions in a climate-constrained world. *Energies* **2019**, *12*, 3870. [\[CrossRef\]](#)
5. Haines, A.; Kovats, R.S.; Campbell-Lendrum, D.; Corvalán, C. Climate change and human health: Impacts, vulnerability and public health. *Public Health* **2006**, *120*, 585–596. [\[CrossRef\]](#)
6. Fadda, J. Climate change: An overview of potential health impacts associated with climate change environmental driving forces. In *Ali Singh Edited Book: Renewable Energy and Sustainable Buildings*; Springer: Cham, Switzerland, 2020; pp. 77–119. [\[CrossRef\]](#)
7. Bureika, G.; Matijošius, J.; Rimkus, A. Alternative Carbonless Fuels for Internal Combustion Engines of Vehicles. In *A Sładkowski Edited Book: Ecology in Transport: Problems and Solutions*; Springer: Cham, Switzerland, 2020; pp. 1–49. [\[CrossRef\]](#)
8. Ni, P.; Wang, X.; Li, H. A review on regulations, current status, effects and reduction strategies of emissions for marine diesel engines. *Fuel* **2020**, *279*, 118477. [\[CrossRef\]](#)
9. Singh, D.; Sharma, D.; Soni, S.L.; Sharma, S.; Kumari, D. Chemical compositions, properties, and standards for different generation biodiesels: A review. *Fuel* **2019**, *253*, 60–71. [\[CrossRef\]](#)
10. Salaheldeen, M.; Mariod, A.A.; Aroua, M.K.; Rahman, S.M.; Soudagar, M.E.M.; Fattah, I.M. Current state and perspectives on transesterification of triglycerides for biodiesel production. *Catalysts* **2021**, *11*, 1121. [\[CrossRef\]](#)
11. Ma, X.; Liu, F.; Helian, Y.; Li, C.; Wu, Z.; Li, H.; Chu, H.; Wang, Y.; Lu, W.; Guo, M.; et al. Current application of MOFs based heterogeneous catalysts in catalyzing transesterification/esterification for biodiesel production: A review. *Energy Convers. Manag.* **2021**, *229*, 113760. [\[CrossRef\]](#)
12. Maheswari, P.; Haider, M.B.; Yusuf, M.; Klemeš, J.J.; Bokhari, A.; Beg, M.; Al-Othman, A.; Kumar, R.; Jaiswal, A.K. A review on latest trends in cleaner biodiesel production: Role of feedstock, production methods, and catalysts. *J. Clean. Prod.* **2022**, *355*, 131588. [\[CrossRef\]](#)
13. Yusoff, M.H.M.; Ayoub, M.; Hamza Nazir, M.; Zahid, I.; Ameen, M.; Abbas, W.; Shoparwe, N.F.; Abbas, N. Comprehensive review on biodiesel production from palm oil mill effluent. *ChemBioEng Rev.* **2021**, *8*, 439–462. [\[CrossRef\]](#)

14. Akyuz, L.; Kaya, M.; Ilk, S.; Cakmak, Y.S.; Salaberria, A.M.; Labidi, J.; Yilmaz, B.A.; Sargin, I. Effect of different animal fat and plant oil additives on physicochemical, mechanical, antimicrobial and antioxidant properties of chitosan films. *Int. J. Biol. Macromol.* **2018**, *111*, 475–484. [CrossRef]
15. Yahaya, W.M.A.W.; Dandan, M.A.; Samion, S.; Musa, M.N. A comprehensive review on palm oil and the challenges using vegetable oil as lubricant base-stock. *J. Adv. Res. Fluid Mech. Therm. Sci.* **2018**, *52*, 182–197. Available online: <https://www.akademiabaru.com/submit/index.php/arfmts/article/view/23891> (accessed on 3 February 2022).
16. Singh, D.; Sharma, D.; Soni, S.L.; Sharma, S.; Sharma, P.K.; Jhalani, A. A review on feedstocks, production processes, and yield for different generations of biodiesel. *Fuel* **2020**, *262*, 116553. [CrossRef]
17. Demirbas, A. *Biodiesel*; Springer: London, UK, 2008; pp. 111–119. [CrossRef]
18. Hong, I.K.; Park, J.W.; Lee, S.B. Optimization of fish-oil-based biodiesel synthesis. *J. Ind. Eng. Chem.* **2013**, *19*, 764–768. [CrossRef]
19. Ravanipour, M.; Hamidi, A.; Mahvi, A.H. Microalgae biodiesel: A systematic review in Iran. *Renew. Sustain. Energy Rev.* **2021**, *150*, 111426. [CrossRef]
20. Lin, C.Y.; Li, R.J. Fuel properties of biodiesel produced from the crude fish oil from the soapstock of marine fish. *Fuel Process. Technol.* **2009**, *90*, 130–136. [CrossRef]
21. Behçet, R. Performance and emission study of waste anchovy fish biodiesel in a diesel engine. *Fuel Process. Technol.* **2011**, *92*, 1187–1194. [CrossRef]
22. Prakash, S.; Prabhakar, M.; Sendilvelan, S.; Venkatesh, R.; Singh, S.; Bhaskar, K. Experimental studies on the performance and emission characteristics of an automobile engine fueled with fish oil methyl ester to reduce environmental pollution. *Energy Procedia* **2019**, *160*, 412–419. [CrossRef]
23. Sharma, P.; Usman, M.; Salama, E.S.; Redina, M.; Thakur, N.; Li, X. Evaluation of various waste cooking oils for biodiesel production: A comprehensive analysis of feedstock. *Waste Manag.* **2021**, *136*, 219–229. [CrossRef]
24. Borah, M.J.; Das, A.; Das, V.; Bhuyan, N.; Deka, D. Transesterification of waste cooking oil for biodiesel production catalyzed by Zn substituted waste egg shell derived CaO nanocatalyst. *Fuel* **2019**, *242*, 345–354. [CrossRef]
25. Bolivar-Telleria, M.; Turbay, C.; Favarato, L.; Carneiro, T.; de Biasi, R.S.; Fernandes, A.A.R.; Santos, A.M.C.; Fernandes, P. Second-generation bioethanol from coconut husk. *BioMed Res. Int.* **2018**, *2018*, 4916497. [CrossRef]
26. Sangkharak, K.; Chookhun, K.; Numreung, J.; Prasertsan, P. Utilization of coconut meal, a waste product of milk processing, as a novel substrate for biodiesel and bioethanol production. *Biomass Convers. Biorefin.* **2020**, *10*, 651–662. [CrossRef]
27. Habibullah, M.; Masjuki, H.H.; Kalam, M.A.; Rahman, S.A.; Mofijur, M.; Mobarak, H.M.; Ashraful, A.M. Potential of biodiesel as a renewable energy source in Bangladesh. *Renew. Sustain. Energy Rev.* **2015**, *50*, 819–834. [CrossRef]
28. Ahmad, A.F.; Zulkurnain, N.; Rosid, S.J.M.; Azid, A.; Endut, A.; Toemen, S.; Ismail, S.; Abdullah, W.N.W.; Aziz, S.M.; Yusoff, N.M.; et al. Catalytic Transesterification of Coconut Oil in Biodiesel Production: A Review. *Catal. Surv. Asia.* **2022**, *26*, 129–143. [CrossRef]
29. Kashyap, S.S.; Gogate, P.R.; Joshi, S.M. Ultrasound assisted synthesis of biodiesel from karanja oil by interesterification: Intensification studies and optimization using RSM. *Ultrason. Sonochem.* **2019**, *50*, 36–45. [CrossRef]
30. Jiaqiang, E.; Pham, M.; Deng, Y.; Nguyen, T.; Duy, V.; Le, D.; Zuo, W.; Peng, Q.; Zhang, Z. Effects of injection timing and injection pressure on performance and exhaust emissions of a common rail diesel engine fueled by various concentrations of fish-oil biodiesel blends. *Energy* **2018**, *149*, 979–989. [CrossRef]
31. Yesilyurt, M.K. The effects of the fuel injection pressure on the performance and emission characteristics of a diesel engine fuelled with waste cooking oil biodiesel-diesel blends. *Renew. Energy* **2019**, *132*, 649–666. [CrossRef]
32. Verma, P.; Sharma, M.P.; Dwivedi, G. Impact of alcohol on biodiesel production and properties. *Renew. Sustain. Energy Rev.* **2016**, *56*, 319–333. [CrossRef]
33. Zareh, P.; Zare, A.A.; Ghobadian, B. Comparative assessment of performance and emission characteristics of castor, coconut and waste cooking based biodiesel as fuel in a diesel engine. *Energy* **2017**, *139*, 883–894. [CrossRef]
34. Rezaia, S.; Oryani, B.; Park, J.; Hashemi, B.; Yadav, K.K.; Kwon, E.E.; Hur, J.; Cho, J. Review on transesterification of non-edible sources for biodiesel production with a focus on economic aspects, fuel properties and by-product applications. *Energy Convers. Manag.* **2019**, *201*, 112155. [CrossRef]
35. Samuel, O.D.; Okwu, M.O. Comparison of Response Surface Methodology (RSM) and Artificial Neural Network (ANN) in modelling of waste coconut oil ethyl esters production. *Energy Source Part A* **2019**, *41*, 1049–1061. [CrossRef]
36. Ong, M.Y.; Nomanbhay, S.; Kusumo, F.; Raja Shahrizzaman, R.M.H.; Shamsuddin, A.H. Modeling and optimization of microwave-based bio-jet fuel from coconut oil: Investigation of Response Surface Methodology (RSM) and Artificial Neural Network Methodology (ANN). *Energies* **2021**, *14*, 295. [CrossRef]
37. Marso, T.M.M.; Kalpage, C.S.; Udugala-Ganehenege, M.Y. ZnO/CuO composite catalyst to pre-esterify waste coconut oil for producing biodiesel in high yield. *React. Kinet. Mech. Catal.* **2021**, *132*, 935–966. [CrossRef]
38. Mahfud, M.; Suryanto, A.; Qadaryah, L.; Suprpto, S.; Kusuma, H.S. Production of methyl ester from coconut oil using microwave: Kinetic of transesterification reaction using heterogeneous CaO catalyst. *Korean Chem. Eng. Res.* **2018**, *56*, 275–280. [CrossRef]
39. Abd Malek, M.N.F.; Pushparaja, L.; Hussin, N.M.; Embong, N.H.; Bhuyar, P.; Rahim, M.H.A.; Maniam, G.P. Exploration of efficiency of nano calcium oxide (CaO) as catalyst for enhancement of biodiesel production. *J. Micro. Biotech. Food Sci.* **2021**, *11*, e3935. [CrossRef]

40. Almeida, L.C.; Barbosa, M.S.; de Jesus, F.A.; Santos, R.M.; Fricks, A.T.; Freitas, L.S.; Pereira, M.M.; Lima, A.S.; Soares, C.M. Enzymatic transesterification of coconut oil by using immobilized lipase on biochar: An experimental and molecular docking study. *Biotechnol. Appl. Biochem.* **2021**, *68*, 801–808. [[CrossRef](#)]
41. Kumar, S.A.; Sakthinathan, G.; Vignesh, R.; Banu, J.R.; Ala'a, H. Optimized transesterification reaction for efficient biodiesel production using Indian oil sardine fish as feedstock. *Fuel* **2019**, *253*, 921–929. [[CrossRef](#)]
42. da Costa Cardoso, L.; de Almeida, F.N.C.; Souza, G.K.; Asanome, I.Y.; Pereira, N.C. Synthesis and optimization of ethyl esters from fish oil waste for biodiesel production. *Renew. Energy* **2019**, *133*, 743–748. [[CrossRef](#)]
43. Kumar, S.; Singhal, M.K.; Sharma, M.P. Utilization of mixed oils for biodiesel preparation: A review. *Energy Sources Part A* **2021**, *43*, 1–34. [[CrossRef](#)]
44. Brahma, S.; Nath, B.; Basumatary, B.; Das, B.; Saikia, P.; Patir, K.; Basumatary, S. Biodiesel production from mixed oils: A sustainable approach towards industrial biofuel production. *Chem. Eng. J. Adv.* **2022**, *10*, 100284. [[CrossRef](#)]
45. Gupta, J.; Agarwal, M.; Dalai, A.K. Optimization of biodiesel production from mixture of edible and nonedible vegetable oils. *Biocatal. Agric. Biotechnol.* **2016**, *8*, 112–120. [[CrossRef](#)]
46. da Costa Barbosa, D.; Serra, T.M.; Meneghetti, S.M.P.; Meneghetti, M.R. Biodiesel production by ethanolsis of mixed castor and soybean oils. *Fuel* **2010**, *89*, 3791–3794. [[CrossRef](#)]
47. Qiu, F.; Li, Y.; Yang, D.; Li, X.; Sun, P. Biodiesel production from mixed soybean oil and rapeseed oil. *Appl. Energy* **2011**, *88*, 2050–2055. [[CrossRef](#)]
48. Razzaq, L.; Abbas, M.M.; Miran, S.; Asghar, S.; Nawaz, S.; Soudagar, M.E.M.; Shaikat, N.; Veza, I.; Khalil, S.; Abdelrahman, A.; et al. Response Surface Methodology and Artificial Neural Networks-Based Yield Optimization of Biodiesel Sourced from Mixture of Palm and Cotton Seed Oil. *Sustainability* **2022**, *14*, 6130. [[CrossRef](#)]
49. Mukherjee, I.; Ray, P.K. A review of optimization techniques in metal cutting processes. *Comput. Ind. Eng.* **2006**, *50*, 15–34. [[CrossRef](#)]
50. GC, M.P.; Krishna, P.; Parappagoudar, M.B. Squeeze casting process modeling by a conventional statistical regression analysis approach. *Appl. Math. Model.* **2016**, *40*, 6869–6888. [[CrossRef](#)]
51. Shadidi, B.; Najafi, G.; Zolfigol, M.A. A Review of the Existing Potentials in Biodiesel Production in Iran. *Sustainability* **2022**, *14*, 3284. [[CrossRef](#)]
52. Said, Z.; Nguyen, T.H.; Sharma, P.; Li, C.; Ali, H.M.; Ahmed, S.F.; Truong, T.H. Multi-attribute optimization of sustainable aviation fuel production-process from microalgae source. *Fuel* **2022**, *324*, 124759. [[CrossRef](#)]
53. Zhang, Y.; Zhong, Y.; Lu, S.; Zhang, Z.; Tan, D. A Comprehensive Review of the Properties, Performance, Combustion, and Emissions of the Diesel Engine Fueled with Different Generations of Biodiesel. *Processes* **2022**, *10*, 1178. [[CrossRef](#)]
54. Sharma, P.; Sahoo, B.B. An ANFIS-RSM based modeling and multi-objective optimization of syngas powered dual-fuel engine. *Int. J. Hydrog Energy* **2022**, *47*, 19298–19318. [[CrossRef](#)]
55. Soudagar, M.E.M.; Afzal, A.; Kareemullah, M. Waste coconut oil methyl ester with and without additives as an alternative fuel in diesel engine at two different injection pressures. *Energy Sources Part A* **2020**, *42*, 1–19. [[CrossRef](#)]
56. Samuel, O.D.; Giwa, S.O.; El-Suleiman, A. Optimization of coconut oil ethyl esters reaction variables and prediction model of its blends with diesel fuel for density and kinematic viscosity. *Biofuels* **2016**, *7*, 723–733. [[CrossRef](#)]
57. Amruth, E.; Sudev, L.J. Optimization of Transesterification Reaction Parameters for Fish Oil Biodiesel Production: A Response Surface Methodology Approach. *J. Phys. Conf. Ser.* **2019**, *1240*, 012140. [[CrossRef](#)]
58. Shettigar, A.K.; Patel, G.C.M.; Chate, G.R.; Vundavilli, P.R.; Parappagoudar, M.B. Artificial bee colony, genetic, back propagation and recurrent neural networks for developing intelligent system of turning process. *SN Appl. Sci.* **2020**, *2*, 1–21. [[CrossRef](#)]
59. Patel, G.C.M.; Jagadish. Experimental modeling and optimization of surface quality and thrust forces in drilling of high-strength Al 7075 alloy: CRITIC and meta-heuristic algorithms. *J. Braz. Soc. Mech. Sci. Eng.* **2021**, *43*, 1–21. [[CrossRef](#)]
60. Venkataramana, S.H.; Shivalingaiah, K.; Davanageri, M.B.; Selvan, C.P.; Lakshmikanthan, A.; Chandrashekarappa, M.P.G.; Razak, A.; Anand, P.B.; Linul, E. Niger Seed Oil-Based Biodiesel Production Using Transesterification Process: Experimental Investigation and Optimization for Higher Biodiesel Yield Using Box–Behnken Design and Artificial Intelligence Tools. *Appl. Sci.* **2022**, *12*, 5987. [[CrossRef](#)]
61. Rangappa, R.; Patel, G.C.M.; Chate, G.R.; Lokare, D.; Lakshmikanthan, A.; Giasin, K.; Pimenov, D.Y. Coaxiality error analysis and optimization of cylindrical parts of CNC turning process. *Int. J. Adv. Manuf. Technol.* **2022**, *120*, 6617–6634. [[CrossRef](#)]
62. Jagadish; Patel, G.C.M.; Sibalija, T.V.; Mumtaz, J.; Li, Z. Abrasive water jet machining for a high-quality green composite: The soft computing strategy for modeling and optimization. *J. Braz. Soc. Mech. Sci. Eng.* **2022**, *44*, 1–20. [[CrossRef](#)]
63. Soto-Mendoza, V.; García-Calvillo, I.; Ruiz-y-Ruiz, E.; Pérez-Terrazas, J. A hybrid grasshopper optimization algorithm applied to the open vehicle routing problem. *Algorithms* **2020**, *13*, 96. [[CrossRef](#)]
64. Heidari, A.A.; Faris, H.; Aljarah, I.; Mirjalili, S. An efficient hybrid multilayer perceptron neural network with grasshopper optimization. *Soft Comput.* **2019**, *23*, 7941–7958. [[CrossRef](#)]
65. Abualigah, L.; Diabat, A. A comprehensive survey of the Grasshopper optimization algorithm: Results, variants, and applications. *Neural. Comput. Appl.* **2020**, *32*, 15533–15556. [[CrossRef](#)]
66. Embong, N.H.; Hindryawati, N.; Bhuyar, P.; Govindan, N.; Rahim, M.H.A.; Maniam, G.P. Enhanced biodiesel production via esterification of palm fatty acid distillate (PFAD) using rice husk ash (NiSO<sub>4</sub>)/SiO<sub>2</sub> catalyst. *Appl. Nanosci.* **2021**, 1–9. [[CrossRef](#)]

67. Ma'arof, N.A.N.B.; Hindryawati, N.; Khazaai, S.N.M.; Bhuyar, P.; Rahim, M.H.A.; Maniam, G.P. Exploitation of cost-effective renewable heterogeneous base catalyst from banana (*Musa paradisiaca*) peel for effective methyl ester production from soybean oil. *Appl. Nanosci.* **2021**, *1*–12. [[CrossRef](#)]
68. Khazaai, S.N.M.; Bhuyar, P.; Rahim, M.H.A.; Alwi, M.H.F.M.; Yiting, S.; Maniam, G.P. Rapid determination of diesel/biodiesel blend ratio using refractive index, density, and kinematic viscosity measurements. *Biomass Convers. Biorefin.* **2021**, *1*–7. [[CrossRef](#)]
69. Mirjalili, S.Z.; Mirjalili, S.; Saremi, S.; Faris, H.; Aljarah, I. Grasshopper optimization algorithm for multi-objective optimization problems. *Appl. Intell.* **2018**, *48*, 805–820. [[CrossRef](#)]
70. Saremi, S.; Mirjalili, S.; Lewis, A. Grasshopper optimisation algorithm: Theory and application. *Adv. Eng. Softw.* **2017**, *105*, 30–47. [[CrossRef](#)]
71. Ashok, A.; Kennedy, L.J.; Vijaya, J.J.; Aruldoss, U. Optimization of biodiesel production from waste cooking oil by magnesium oxide nanocatalyst synthesized using coprecipitation method. *Clean Technol. Environ. Policy* **2018**, *20*, 1219–1231. [[CrossRef](#)]
72. Abdullah, R.F.; Rashid, U.; Ibrahim, M.L.; Hazmi, B.; Alharthi, F.A.; Nehdi, I.A. Bifunctional nano-catalyst produced from palm kernel shell via hydrothermal-assisted carbonization for biodiesel production from waste cooking oil. *Renew. Sustain. Energy Rev.* **2021**, *137*, 110638. [[CrossRef](#)]
73. Abusweireh, R.S.; Rajamohan, N.; Vasseghian, Y. Enhanced production of biodiesel using nanomaterials: A detailed review on the mechanism and influencing factors. *Fuel* **2022**, *319*, 123862. [[CrossRef](#)]
74. Farooq, M.; Ramli, A.; Subbarao, D. Biodiesel production from waste cooking oil using bifunctional heterogeneous solid catalysts. *J. Clean. Prod.* **2013**, *59*, 131–140. [[CrossRef](#)]
75. Chen, G.Y.; Shan, R.; Yan, B.B. Remarkably enhancing the biodiesel yield from palm oil upon abalone shell-derived CaO catalysts treated by ethanol. *Fuel Process. Technol.* **2016**, *143*, 110–117. [[CrossRef](#)]
76. Wen, Z.; Yu, X.; Tu, S.T.; Yan, J.; Dahlquist, E. Synthesis of biodiesel from vegetable oil with methanol catalyzed by Li-doped magnesium oxide catalysts. *Appl. Energy* **2010**, *87*, 743–748. [[CrossRef](#)]
77. Hebbar, H.H.; Math, M.C.; Yatish, K.V. Optimization and kinetic study of CaO nano-particles catalyzed biodiesel production from Bombax ceiba oil. *Energy* **2018**, *143*, 25–34. [[CrossRef](#)]
78. Munir, M.; Ahmad, M.; Mubashir, M.; Asif, S.; Waseem, A.; Mukhtar, A.; Saqib, S.; Munawaroh, H.S.H.; Lam, M.K.; Khoo, K.S.; et al. A practical approach for synthesis of biodiesel via non-edible seeds oils using trimetallic based montmorillonite nano-catalyst. *Bioresour. Technol.* **2021**, *328*, 124859. [[CrossRef](#)]
79. Foroutan, R.; Mohammadi, R.; Esmaeili, H.; Bektashi, F.M.; Tamjidi, S. Transesterification of waste edible oils to biodiesel using calcium oxide@ magnesium oxide nanocatalyst. *Waste Manag.* **2020**, *105*, 373–383. [[CrossRef](#)]
80. Baskar, G.; Selvakumari, I.A.E.; Aiswarya, R.J.B.T. Biodiesel production from castor oil using heterogeneous Ni doped ZnO nanocatalyst. *Bioresour. Technol.* **2018**, *250*, 793–798. [[CrossRef](#)]
81. Rasouli, H.; Esmaeili, H. Characterization of MgO nanocatalyst to produce biodiesel from goat fat using transesterification process. *3 Biotech* **2019**, *9*, 1–11. [[CrossRef](#)]
82. Changmai, A.; Rano, R.; Vanlaveni, C.; Rokhum, L. A novel Citrus sinensis peel ash coated magnetic nanoparticles as an easily recoverable solid catalyst for biodiesel production. *Fuel* **2021**, *286*, 119447. [[CrossRef](#)]
83. Patel, G.C.M.; Shettigar, A.K.; Parappagoudar, M.B. A systematic approach to model and optimize wear behaviour of castings produced by squeeze casting process. *J. Manuf. Process.* **2018**, *32*, 199–212. [[CrossRef](#)]
84. Patel, G.C.M.; Krishna, P.; Parappagoudar, M.B.; Vundavilli, P.R. Multi-objective optimization of squeeze casting process using evolutionary algorithms. *Int. J. Swarm Intell. Res.* **2016**, *7*, 55–74. [[CrossRef](#)]
85. Saffari, A.; Zahiri, S.H.; Khishe, M. Fuzzy grasshopper optimization algorithm: A hybrid technique for tuning the control parameters of GOA using fuzzy system for big data sonar classification. *Iran. J. Electr. Electron. Eng.* **2022**, *18*, 2131. [[CrossRef](#)]
86. Malek, M.N.F.A.; Hussin, N.M.; Embong, N.H.; Bhuyar, P.; Rahim, M.H.A.; Govindan, N.; Maniam, G.P. Ultrasonication: A process intensification tool for methyl ester synthesis: A mini review. *Biomass Convers. Biorefin.* **2020**, *1*–11. [[CrossRef](#)]
87. Jung, S.; Kim, M.; Lin, K.Y.A.; Park, Y.K.; Kwon, E.E. Biodiesel synthesis from bio-heavy oil through thermally induced transesterification. *J. Clean. Prod.* **2021**, *294*, 126347. [[CrossRef](#)]
88. da Silva Dutra, L.; Pinto, M.C.C.; Cipolatti, E.P.; Aguiéiras, E.C.G.; Manoel, E.A.; Greco-Duarte, J.; Freiere, D.M.G.; Pinto, J.C. How the biodiesel from immobilized enzymes production is going on: An advanced bibliometric evaluation of global research. *Renew. Sustain. Energy Rev.* **2022**, *153*, 111765. [[CrossRef](#)]
89. Liganiso, E.C.; Tlhaole, B.; Magagula, L.P.; Dziike, S.; Liganiso, L.Z.; Motaung, T.E.; Moloto, N.; Tetana, Z.N. Biodiesel production from waste oils: A South African outlook. *Sustainability* **2022**, *14*, 1983. [[CrossRef](#)]
90. Changmai, B.; Sudarsanam, P.; Rokhum, L. Biodiesel production using a renewable mesoporous solid catalyst. *Ind. Crops Prod.* **2020**, *145*, 111911. [[CrossRef](#)]
91. Yahyae, R.; Ghobadian, B.; Najafi, G. Waste fish oil biodiesel as a source of renewable fuel in Iran. *Renew. Sustain. Energy Rev.* **2013**, *17*, 312–319. [[CrossRef](#)]
92. Keera, S.T.; El Sabagh, S.M.; Taman, A.R. Castor oil biodiesel production and optimization. *Egypt. J. Pet.* **2018**, *27*, 979–984. [[CrossRef](#)]
93. Abed, K.A.; El Morsi, A.K.; Sayed, M.M.; El Shaib, A.A.; Gad, M.S. Effect of waste cooking-oil biodiesel on performance and exhaust emissions of a diesel engine. *Egypt. J. Pet.* **2018**, *27*, 985–989. [[CrossRef](#)]

- 
94. Ewunie, G.A.; Morken, J.; Lekang, O.I.; Yigezu, Z.D. Factors affecting the potential of *Jatropha curcas* for sustainable biodiesel production: A critical review. *Renew. Sustain. Energy Rev.* **2021**, *137*, 110500. [[CrossRef](#)]
  95. Zahan, K.A.; Kano, M. Biodiesel production from palm oil, its by-products, and mill effluent: A review. *Energies* **2018**, *11*, 2132. [[CrossRef](#)]